Quarterly Technical Report

Selected Energy Epitaxial Deposition and Low Energy Electron Microscopy of AlN, GaN and SiC Thin Films

Supported under Grant #N00014-95-1-0122
Office of the Chief of Naval Research
Report for the period 10/1/97–12/31/97

R. F. Davis, H. H. Lamb† and I. S. T. Tsong*,
E. Bauer*, E. Chen†, R. B. Doak*, J. L. Edwards*,
N. Freed*, J. Fritsch*, D. C. Jordan*, A. Michel†,
A. Pavlovska*, K. E. Schmidt*, and V. Torres*
Materials Science and Engineering Department
†Chemical Engineering
North Carolina State University
Campus Box 7907
Raleigh, NC 27695-7907
and
*Department of Physics and Astronomy
Arizona State University
Tempe, AZ 85287-1504

December, 1997

REPORT DOCUMENTATION PAGE

Form Approved
OMB No. 0704-0188

1. AGENCY USE ONLY *(Leave blank)*	2. REPORT DATE	3. REPORT TYPE AND DATES COVERED
	December, 1997	Quarterly Technical 10/1/97–12/31/97

4. TITLE AND SUBTITLE

Selected Energy Epitaxial Deposition and Low Energy Electron Microscopy of AlN, GaN, and SiC Thin Films

5. FUNDING NUMBERS

1213801---01
312
N00179
N66020
4B855

6. AUTHOR(S)

R. F. Davis, H. H. Lamb and I. S. T. Tsong

7. PERFORMING ORGANIZATION NAME(S) AND ADDRESS(ES)

North Carolina State University
Hillsborough Street
Raleigh, NC 27695

8. PERFORMING ORGANIZATION REPORT NUMBER

N00014-95-1-0122

9. SPONSORING/MONITORING AGENCY NAMES(S) AND ADDRESS(ES)

Sponsoring: ONR, Code 312, 800 N. Quincy, Arlington, VA 22217-5660
Monitoring: Administrative Contracting Officer, Regional Office Atlanta
Atlanta Regional Office
100 Alabama Street, Suite 4R15
Atlanta, GA 30303

10. SPONSORING/MONITORING AGENCY REPORT NUMBER

11. SUPPLEMENTARY NOTES

12a. DISTRIBUTION/AVAILABILITY STATEMENT

Approved for Public Release; Distribution Unlimited

12b. DISTRIBUTION CODE

13. ABSTRACT ***(Maximum 200 words)***

LEEM/LEED studies were conducted on 6H-SiC(0001) substrates etched in different environments including: (a) pure hydrogen at atmospheric pressure at 1600°C; (b) a mixture of HCl and hydrogen at 1350°C; and (c) a mixture of 5% hydrogen in atmospheric helium at 1600°C. Substrates with reasonable stepped structures and suitable for *in situ* LEEM studies of nitride film growth were obtained after using technique (c). Effective dissociation and adsorption mechanisms during the impact of ammonia molecules on the polar and nonpolar surfaces of GaN were identified by analyzing trajectories obtained from short-period molecular-dynamics simulations. The co-adsorption of NH_2 and H is exothermic for the case where NH_2 binds to cation dangling bonds and H binds to anion dangling bonds of the surface. The energy barrier for the dissociative adsorption of ammonia on the GaN(000$\bar{1}$) surface is estimated to be smaller than 0.5 eV. It was also determined that ammonia physisorbs on this surface at low kinetic energies (i.e. 0.031-0.061 eV). Dissociative chemisorption is initiated with increasing kinetic energy. For kinetic energies greater than 0.33 eV, the growth rate remains constant suggesting that the barrier for dissociative chemisorption has been overcome. From these observations it is proposed that the barrier height is approximately 0.3±0.1 eV. Preliminary results suggest that AlN films grown on hydrogen etched SiC substrates are superior to those grown on as-received SiC substrates. Homoepitaxial growth of GaN on OMVPE-grown GaN/AlN/SiC substrates was accomplished using a NH_3-seeded supersonic molecular beam and Ga effusion cell. Gallium-limited growth kinetics were observed at 730 and 770°C for incident Ga fluxes $\leq 1.2\times10^{15}$ $cm^{-2}s^{-1}$ using a 0.25 eV NH_3 beam. The Ga incorporation efficiency was 20-25%; the growth rate was nearly independent of substrate temperature.Increasing the NH_3 kinetic energy within the 0.25 to 0.61 eV range resulted in a modest increase in the GaN growth rate as a result of enhanced NH_3 reactivity. A concomitant increase in surface roughness was observed with increasing GaN growth rate. Higher substrate temperatures negated the effects of incident kinetic energy on growth rate and film morphology.

14. SUBJECT TERMS

LEEM, LEED, 6H-SiC(0001), etching, hydrogen, HCl, homoepitaxial growth, molecular beam, incorporation efficiency, surface roughness, growth kinetics, morphology, dissociation, adsorption, surface, molecular-dynamics, dissociative chemisorption, kinetic energy, barrier height

15. NUMBER OF PAGES

27

16. PRICE CODE

17. SECURITY CLASSIFICATION OF REPORT	18. SECURITY CLASSIFICATION OF THIS PAGE	19. SECURITY CLASSIFICATION OF ABSTRACT	20. LIMITATION OF ABSTRACT
UNCLAS	UNCLAS	UNCLAS	SAR

Table of Contents

I. Introduction

The realized and potential electronic applications of AlN, GaN and SiC are well known. Moreover, a continuous range of solid solutions and pseudomorphic heterostructures of controlled periodicities and tunable band gaps from 2.3 eV (3C-SiC) to 6.3 eV (AlN) have been produced at North Carolina State University (NCSU) and elsewhere in the GaN-AlN and AlN-SiC systems. The wide band gaps of these materials and their strong atomic bonding have allowed the fabrication of high-power, high-frequency and high-temperature devices. However, the high vapor pressures of N and Si in the nitrides and SiC, respectively, force the use of low deposition temperatures with resultant inefficient chemisorption and reduced surface diffusion rates. The use of these low temperatures also increases the probability of the uncontrolled introduction of impurities as well as point, line and planar defects which are likely to be electrically active. An effective method must be found to routinely produce intrinsic epitaxial films of AlN, GaN and SiC having low defect densities.

Recently, Ceyer [1, 2] has demonstrated that the barrier to dissociative chemisorption of a reactant upon collision with a surface can be overcome by the translational energy of the incident molecule. Ceyer's explanation for this process is based upon a potential energy diagram (Fig. 1) similar to that given by classical transition-state theory (or activated-complex theory) in chemical kinetics. The dotted and dashed lines in Fig. 1 show, respectively, the potential wells for molecular physisorption and dissociative chemisorption onto the surface. In general, there will be an energy barrier to overcome for the atoms of the physisorbed molecule to dissociate and chemically bond to the surface. Depending upon the equilibrium positions and well depths of the physisorbed and chemisorbed states, the energy of the transition state E^* can be less than zero or greater than zero. In the former case, the reaction proceeds spontaneously. In the latter case, the molecule will never proceed from the physisorbed state (the precursor state) to the chemisorbed state unless an additional source of energy can be drawn upon to surmount the barrier. This energy can only come from either (1) the thermal energy of the surface, (2) stored internal energy (rotational and vibrational) of the molecule, or (3) the incident translational kinetic energy of the molecule. Conversion of translational kinetic energy into the required potential energy is the most efficient of these processes. Moreover, by adjusting the kinetic energy, Ei, of the incoming molecule, it is possible to turn off the reaction ($Ei < E^*$), to tailor the reaction to just proceed ($Ei = E^*$), or to set the amount of excess energy to be released ($Ei > E^*$). The thrust of the present research is to employ these attributes of the beam translational energy to tune the reaction chemistry for wide band gap semiconductor epitaxial growth.

The transition state, E^*, is essentially the activation energy for dissociation and chemisorption of the incident molecules. Its exact magnitude is unknown, but is most certainly

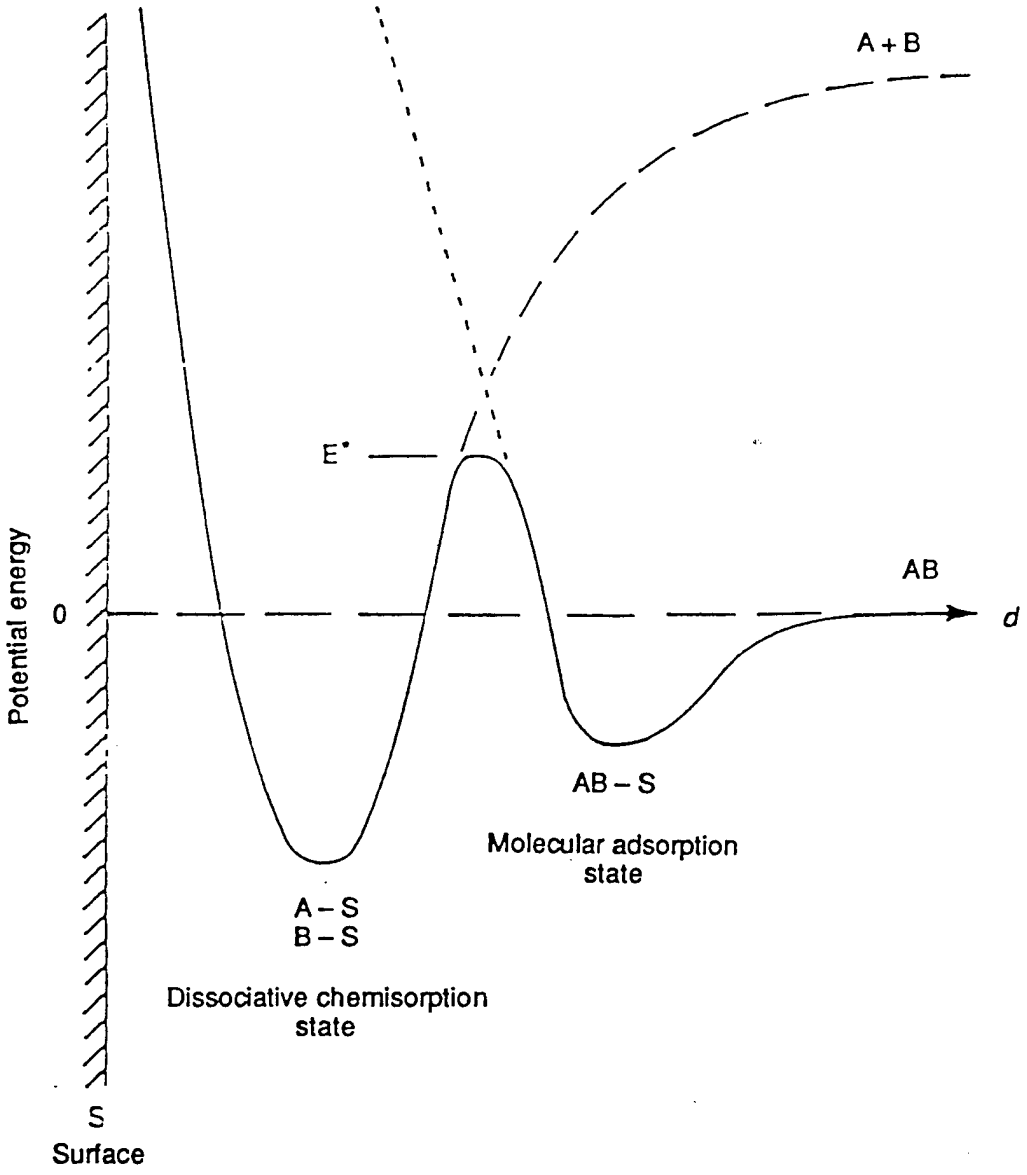

Figure 1. Schematic potential energy diagram of an activated surface reaction involving a molecularly physisorbed precursor state [from Ref. 1].

lower than the dissociation energy of the free molecule. It does not necessarily follow, however, that any kinetic energy above E* will promote high-quality epitaxial growth of GaN. One must take into consideration another energy threshold, Ed, beyond which the kinetic energy of the incident flux will cause damage to the epitaxial film being synthesized. A typical Ed threshold value is approximately five times the bandgap of the crystal and in the case of GaN, Ed ≈18 eV.

From the above consideration, it is clear that the key to high quality epitaxial growth is to be able to tune the energy of the incoming flux species over a range of energies defined by the window between E* and Ed. Since the window is quite restrictive, i.e. 1-20 eV, it is essential that the energy spread of the flux species must be small, i.e. the flux species should ideally be

monoenergetic. To this end, we employ selected energy epitaxial deposition (SEED) systems for the growth of AlN, GaN and SiC wide band gap semiconductors. The SEED systems are of two types: (1) a seeded-beam supersonic free-jet (SSJ) and (2) a dual ion-beam Colutron. Both these SEED systems have the desirable property of a narrow energy spread of ≤ 1 eV.

Epitaxial growth using the seeded-beam SSJ involves a close collaboration between investigators at NCSU and Arizona State University (ASU). At ASU, the SSJ is interfaced directly into a low-energy electron microscope (LEEM) for the conduct of *in situ* studies of the nucleation and growth of epitaxial layers; while at NCSU, the SSJ systems are used to grow device-quality AlN, GaN and SiC for real applications. Exchanges in personnel (students) and information between the two groups ensures the achievement of desired results. The additional thin film growth experiments using dual-beam Colutrons and the theoretical studies referred to in this report are primarily conducted at ASU.

The research conducted in this reporting period and described in the following sections has been concerned with (1) etching in different environments and the effect on surface morphology of 6H-SiC(0001) substrates prepared for LEEM studies, (2) chemical reactions of ammonia with polar and nonpolar GaN surfaces, (3) effects of energy and angle of incidence on AlN and GaN epitaxial growth using He supersonic beams seeded with ammonia, and (4) homoepitaxial growth of GaN films using ammonia-seeded supersonic beams. The following individual sections detail the procedures, results, discussions of these results, conclusions and plans for future research. Each subsection is self-contained with its own figures, tables and references.

1. S. T. Ceyer, Langmuir 6, 82 (1990).
2. S. T. Ceyer, Science 249, 133 (1990).

II. Surface Morphology of 6H-SiC(0001) Substrates Prepared for LEEM Studies of Nitride Film Growth

In the past, different approaches have been attempted to obtain clean, flat, and scratch-free 6H-SiC(0001) substrates for the epitaxial growth of nitride films, and for LEEM studies of these growths. Various *ex situ* etching procedures described in previous reports have not yielded to the desired result of minimizing the surface defects in commercially available SiC and, in addition, producing a surface ideal for LEEM examination. In order to conduct useful growth studies in the LEEM, the surface preparation procedures must lead to a controlled and consistent surface in a reproducible manner.

A dilute hydrogen etch, modeled after Chu and Campbell [1] and Harris *et al.*[2] (subsequently used by Prof. Feenstra's group at Carnegie Mellon University) was developed in house. The tests showed that the dilute hydrogen-etch technique had the potential to consistently produce SiC surfaces satisfactory for Group III nitride deposition. The 6H-SiC(0001) surface was exposed to a 5% hydrogen in helium mixture at a temperature of 1600°C for times ranging from five to thirty minutes. The samples were heated by a RF coupled molybdenum susceptor in the mixed gas at a flow rate of approximately 100 cc/minute. Samples treated by this process were examined in the LEEM to compare them with SiC substrates treated by D. J. Larkin of NASA Lewis and by Feenstra's group at CMU.

This etch was very safe to use because pure hydrogen was not used and the concentration was well below the explosion limit. However, the results appeared to be identical to those achieved with pure hydrogen treatment at CMU. There were some notable differences between the hydrogen-etched samples (ASU and CMU) and the HCl/H_2 etched samples at 1350°C (NASA Lewis). The details are given below.

As reported in the June 1997 Quarterly Report, some of the CMU-cleaned SiC crystals were observed to have irregular rounded inclusions which looked like etch pits. Upon heating to high temperatures, a 3×3 LEED pattern developed in these areas, characteristic for C-termination, while in the regions with good step structure the weak and diffuse $\sqrt{3}$ pattern became much sharper and more intense just before graphitization occurred. The crystals studied in this report period showed only the $\sqrt{3}$ pattern with the same sharpening and intensification as the "good" regions in the CMU-cleaned crystals before graphitization. This suggested that the "adatoms" of the $\sqrt{3}$ structure on the Si-terminated surface (whose nature is still an open question in the literature) are C atoms or clusters and that the $\sqrt{3}$ structure was a precursor to graphite formation.

While no dramatic variations between the LEED patterns of the differently-prepared crystals (NASA Lewis and ASU) were noticed, major differences were seen in the LEEM images. The crystals treated by NASA Lewis had a large number of etch pits with two typical configurations

which are shown in Fig. 1 while the ASU-cleaned crystals had far fewer etch pits. The step structure of the NASA-cleaned crystals was very complex, as illustrated by Fig 2, that of the ASU-cleaned crystals was simple and very regular, very similar to that of the "good" CMU-cleaned crystals. However, in contrast to the CMU-cleaned crystals, they showed many linear defects oriented in three equivalent crystal directions independent of step spacing (Fig. 3). The NASA-cleaned crystals have steps of different height (Fig. 2a) and showed step orientation-dependent faceting (Figs. 2b and d). Faceted and unfaceted steps can, however, also have the same orientation (Fig. 2c).

The thermal stability of the SiC surface as characterized by the intensification and sharpening of the $\sqrt{3}$ LEED spots and by the change of the surface morphology as seen by LEEM seemed to be higher than reported in the literature. The temperature was measured with a thermocouple spot-welded to the W disk against which the crystal was pressed and by an infrared optical pyrometer operating at a wavelength of 5 μm, using an emissivity factor of 0.5. Both were calibrated by measuring the Si(111) phase transition temperature (840°C) of a Si crystal mounted in the same manner. The $\sqrt{3}$ improvement occurred typically around 1100°C, the onset of graphitization about 100°C higher upon brief (less than 1 min.) heating to these temperatures. These temperatures depended somewhat upon the sample morphology and its prehistory. Figures 4a and 4b illustrate the transition from the $\sqrt{3}$ structure to the graphitic layer on an ASU-cleaned crystal, Figs. 4c and 4d show the early stages of graphitization of a NASA-cleaned crystal and Fig. 5a, a CMU-cleaned crystal just before graphitization showing the strong $\sqrt{3}$ LEED pattern of Fig. 5b. It was obvious that the best $\sqrt{3}$ pattern occurred when the surface changed its morphology. Graphitization, as seen in LEED, was connected with the appearance of patches which appeared dark in Fig. 4, but bright at other energies. Much smaller regions of this type were already present in Fig. 5.

The images shown here were selected from more than 50 hours of video tape with the goal of showing the most characteristic features. Many other features have been recorded and observed, demonstrating a bewildering morphological variety. This study was, by necessity, of a statistical nature, in part because there was no control over the cleaning procedures used by our collaborators and in part because the crystals were from different shipments over a period of several years during which the suppliers improved the quality of their crystals. A systematic study of the influence of the cleaning process requires a well-documented, reproducible cleaning procedure and crystals from the same batch. However, irreproducibilities may still occur due to local variations of the type and concentration of imperfections such as polytype inclusions, micropipes and dislocations. Nevertheless, it is hoped that a careful protocol for each crystal will allow future systematic studies of SiC surfaces so that the growth of nitrides on them can be studied more quantitatively.

References

1. T. L. Chu and R. B. Campbell, J. Electrochem. Soc. **112**, 955 (1965).
2. J. J. Harris, H. C. Gatos, and A. F. Witt, J. Electrochem. Soc. **116**, 380 (1969).

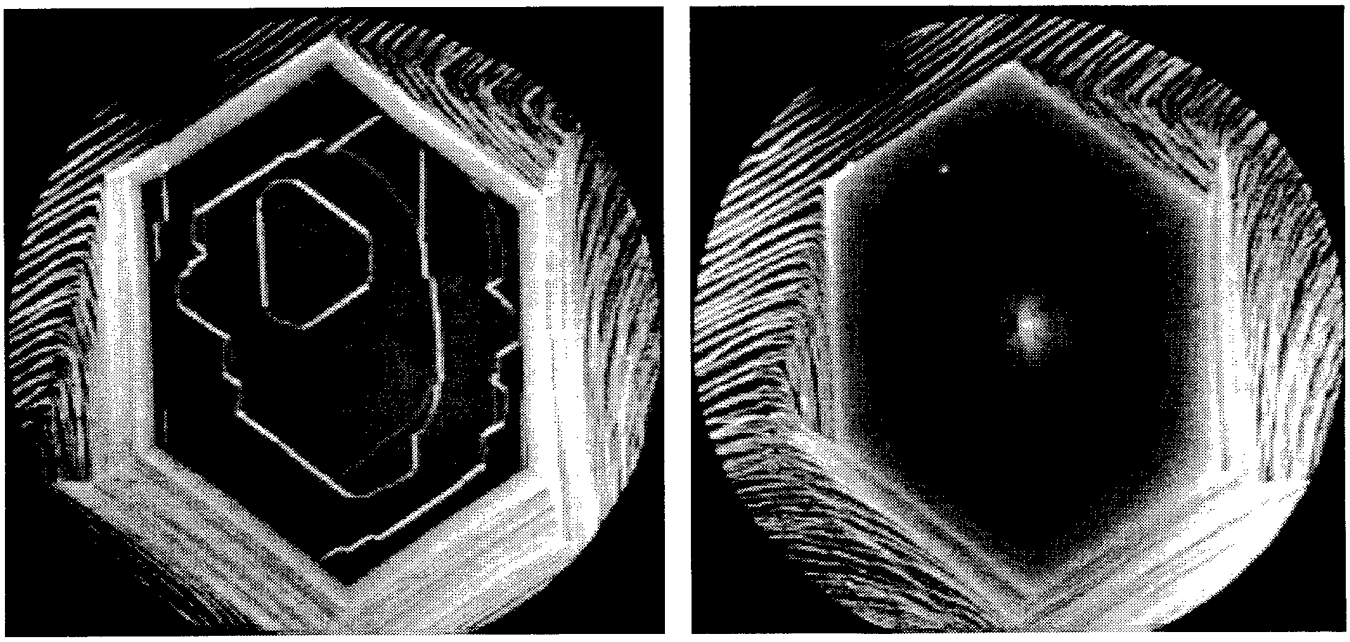

Figure 1. Typical etch pits on the NASA-cleaned 6H-SiC(0001) surface. Field of view 26 μm, electron energy 7.0 eV (a) and 4.3 eV (b).

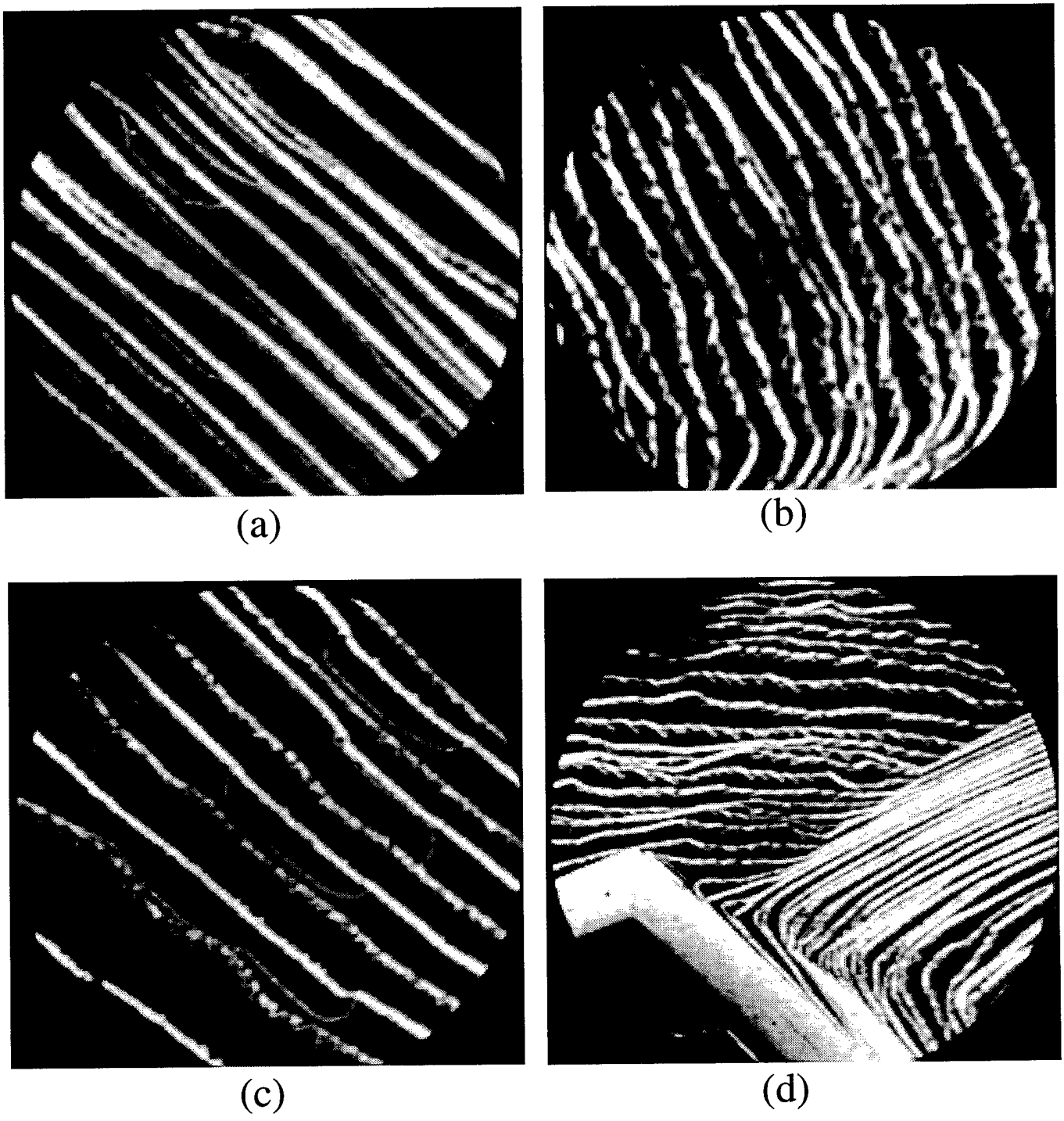

Figure 2. Typical step structures on the NASA-cleaned 6H-SiC(0001) surface. Field of view 4.8 μm, electron energy 7.0 eV. Same crystal as in Fig. 1.

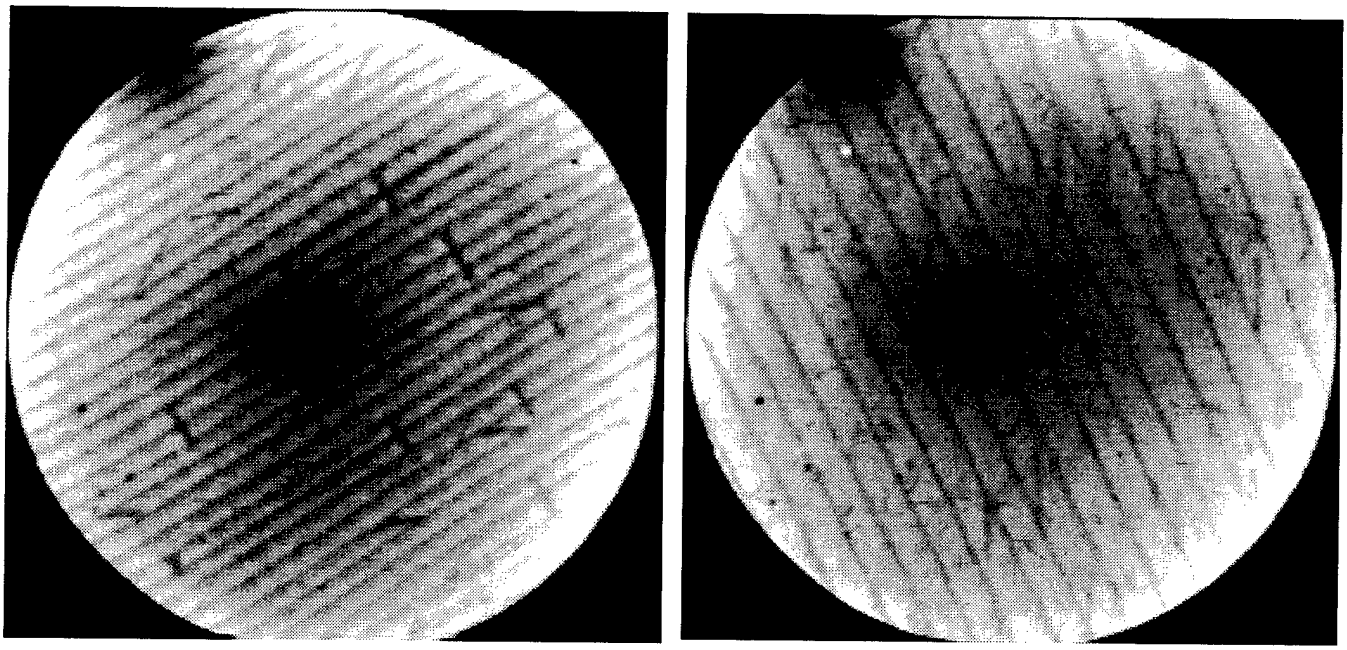

(a) (b)

Figure 3. Typical step structures on the ASU-cleaned 6H-SiC(0001) surfaces, showing linear defects. Field of view 4.8 μm, electron energy 14.4 eV (a) and 5.7 eV (b) Two different crystals.

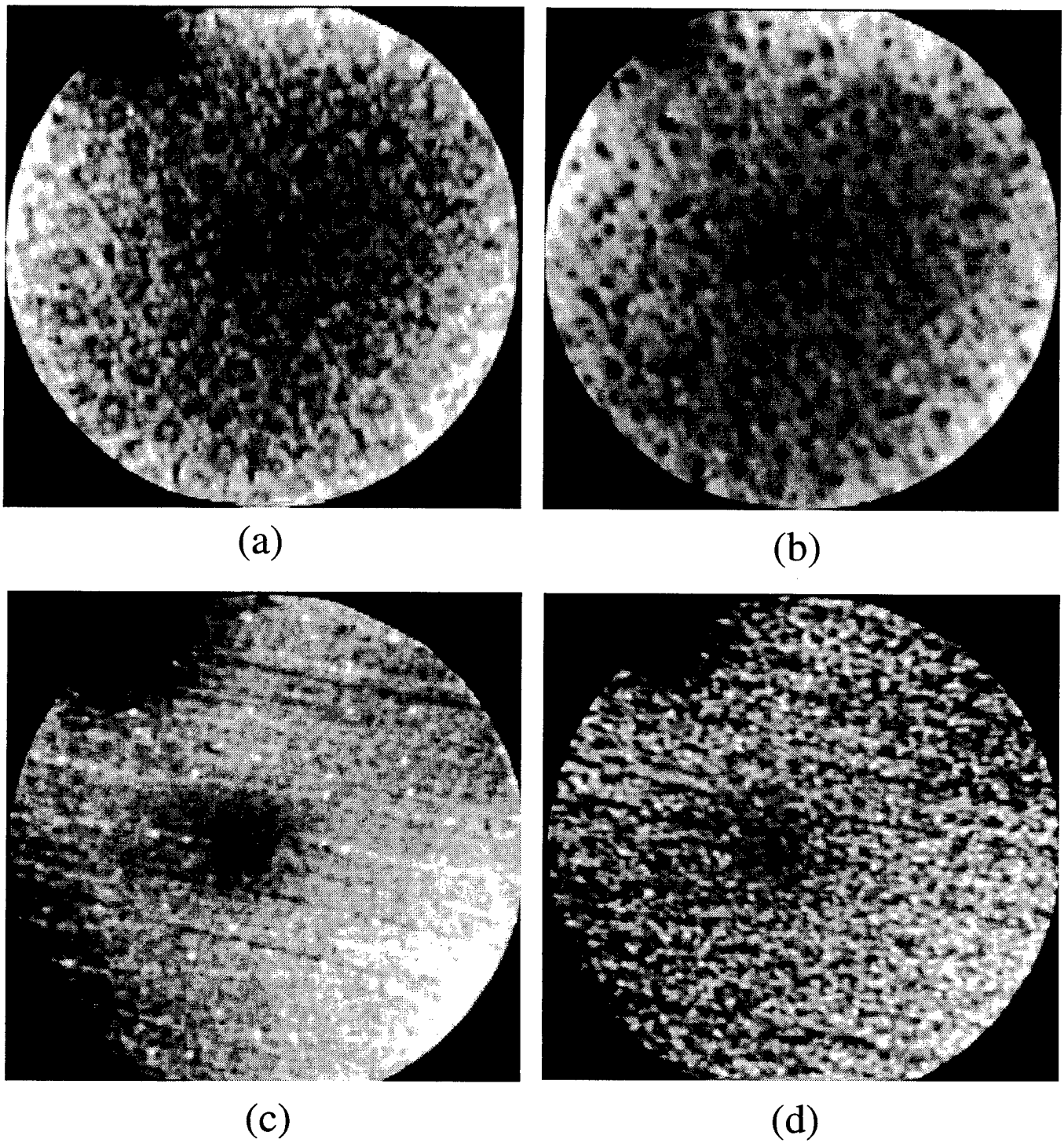

Figure 4. Morphology of an ASU-cleaned crystal (a,b) and of a NASA-cleaned crystal (c,d): (a) after heating resulting in the sharp strong $\sqrt{3}$ structure and (b) in the early stages of graphite layer formation; (c,d) at two different stages of graphite layer formation. Field of view 4.8 μm, electron energy 8.0 eV (a,b), 11.7 eV (c) and 8.2 eV (d).

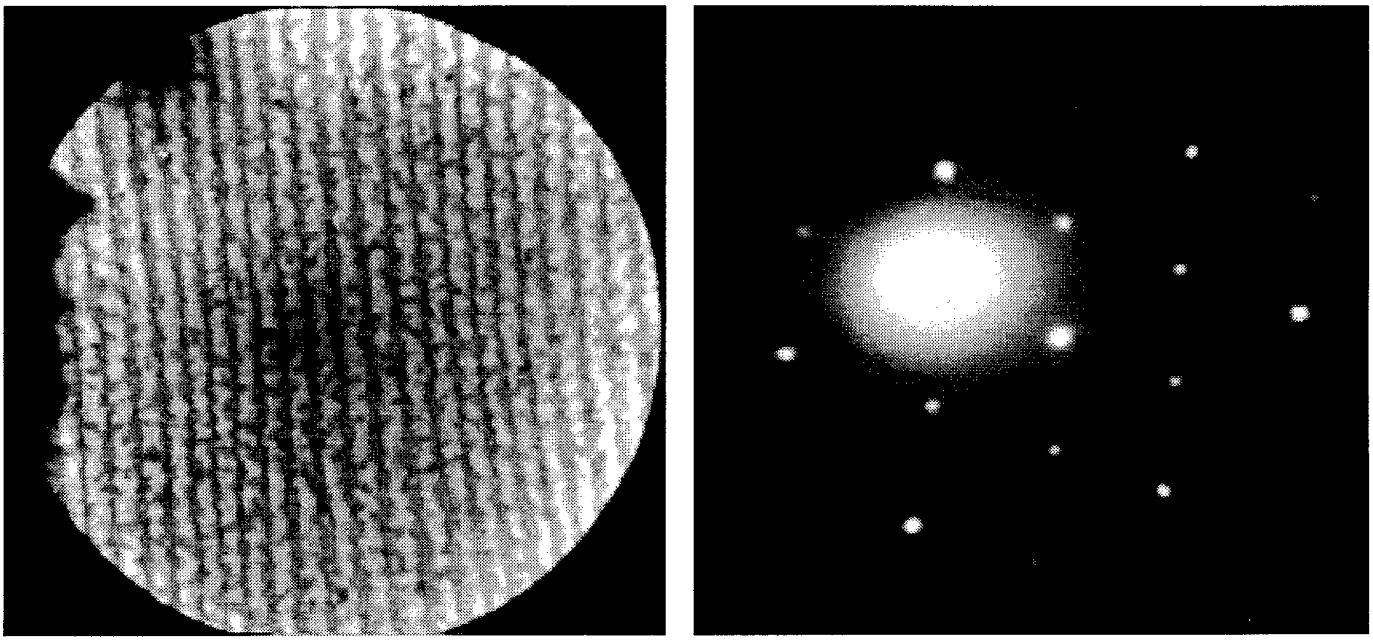

a b

Figure 5. Morphology of a CMU-cleaned crystal after heating leading to a sharp strong $\sqrt{3}$ structure. (a) LEEM image, field of view 4.8 μm, electron energy 34.2 eV (b) LEED $\sqrt{3} \times \sqrt{3}$ pattern, electron energy 40.8 eV.

III. Chemical Reactions of Ammonia with Polar and Nonpolar Nitride Semiconductor Surfaces

It was proven recently that thin GaN and AlN films can be successfully fabricated using supersonic He-atom beams seeded with ammonia molecules [1]. This technique allows one to deposit NH_3 under well-defined conditions including the translational energy of the molecules, their angle of incidence, and the substrate temperature. Hence, energy barriers relevant for dissociation and chemisorption processes can be probed in great detail by means of seeded beam experiments. Here, results are presented from the *ab initio* local-orbital calculations [2, 3] performed to study the impact of ammonia on GaN. The focus was on chemical reactions on the nonpolar $(10\bar{1}0)$ and $(10\bar{2}0)$ and the polar (0001) surfaces of GaN. The dissociation barrier was determined for the adsorption on GaN$(000\bar{1})$ by computing the potential energy surface. Energy differences were given with respect to a free ammonia molecule above the respective surface structure. The local-orbital formalism yielded 1.134 Å for the N-H bond-length and 109.8° for the H-N-H bond-angle, while the experimental values were 1.012 Å and 106.7° [4].

Co-adsorption of NH_2 and H on Nonpolar GaN Surfaces

First, the dissociative adsorption of NH_3 on the non-polar GaN$(10\bar{1}0)$ surface is discussed. The calculations were carried out for crystal films spanning five atomic layers. The atoms in bottom layer of the slab-supercell were kept in the bulk-derived positions, and their dangling bonds were saturated with hydrogen. All other atoms in the system were allowed to relax.

The adsorption of NH_2 and H from a dissociated ammonia molecule was exothermic for the case that hydrogen bound to the nitrogen atom and NH_2 to the gallium atom of the same Ga-N pair on the surface (NH_2-Ga configuration). The chemisorption of one NH_2 and H per (1×2) surface decreased the total energy by 1.56 eV. In contrast, the total energy was increased by 1.19 eV, if NH_2 bound to the surface nitrogen and hydrogen saturated the gallium dangling bond (NH_2-N configuration). For the coverage of all Ga-N pairs on the $(10\bar{1}0)$ surface with NH_2 and H, the energy decrease computed for the formation of the NH_2-Ga configuration was 1.95 eV, while the energy increase obtained for the NH_2-N configuration was 0.81 eV. The energy gain of 1.95 eV compared very well with 2.08 eV recently determined in a plane-wave calculation [4].

Also considered was the co-adsorption of NH_2 and H on the GaN$(10\bar{2}0)$ surface. The total energy was lowered by about 1.0 eV if NH_2 chemisorbs on a Ga-dangling bond and H bound to either of the two neighboring surface N-dangling bonds. The formation of the NH_2-N chemisorption system increased the total energy by 1.78 eV. As for the case of the $(10\bar{1}0)$ surface, the energy of the NH_2-Ga configuration was found to be lower by about 2.75 eV,

compared to that for the NH_2-N adsorption system. The energy gain resulting from the NH_2-Ga configuration originated from the fact that the number of bonds in the system was increased without reducing the number of N-H bonds. The adsorption of the NH_2 group led to one additional Ga-N bond. In contrast, the total energy was increased through the formation of the NH_2-N configuration, since NH bonds were replaced by Ga-H bonds.

Co-adsorption of NH_2 and H on GaN($000\bar{1}$)

For the investigation of possible pathways of ammonia reacting with the (0001) surfaces of GaN, many different situations were considered. The experiments of Refs. [5] and [6] gave evidence for a nominally anion-terminated GaN($000\bar{1}$) surface, while the appearance of flat cationterminated and rough anion-terminated facets were reported in Refs. [7] and [8]. Hence, nitrogen adsorption processes have to be analyzed for both of the two surface polarities.

The dissociative adsorption of ammonia was investigated on the vacancy structure of the GaN($000\bar{1}$) surface, which was chosen as a possible scenario. Figures 1 and 2 illustrate a minimum-energy pathway determined for the chemisorption process. The ammonia molecule split into NH_2 and H The NH_2 group bind to two of the three second-layer Ga atoms neighboring the vacancy, while the dissociating H bound to a first-layer nitrogen atom. This reaction lowered the total energy of the system by 2.05 eV.

The adsorption mechanism and its energy barrier were determined by means of total energy calculations performed for a large variety of different configurations of the molecule. As in the computations for the (0001) surface structures, a $p(2\times2)$ slab-supercell with five atomic bilayers was used. The atomic positions on both sides of the crystal film were relaxed into the equilibrium positions of the respective vacancy structures prior to the investigation of the chemisorption mechanism. The adsorption of one molecule per $p(2x2)$ unit cell was considered. Total energy differences were calculated with respect to the energy of the pristine surface and a NH_3 molecule in vacuum.

To obtain a parameterization for the reaction coordinate, the molecular-dynamics trajectory for an impact of ammonia on the nitrogen vacancy, which led to the formation of the co-adsorption configuration was analyzed. From the trajectory, information about the transition state and reactive surface sites was extracted. Ammonia reached the transition state by approaching the vacancy structure above position 1, as illustrated in Fig. 1. The dissociation of one hydrogen from the molecule was supported by the formation of new bonds. The new H-N bond led to a relaxation of the separated hydrogen to the on-top bonding site of the nearest first-layer nitrogen atom (denoted as 2' in Fig. 1), while the nitrogen of the NH_2 group established chemical bonds with two second layer Ga atoms by moving closer to the surface and to the lateral position labeled as 2 in Fig. 1.

The parameterization of the reaction mechanism is illustrated in Fig 2b The parameter λ_N defined the lateral position of the nitrogen between sites 1 ($\lambda_N = 0.0$) and 2 ($\lambda_N = 1.0$). In addition, the vertical distance z_N of the nitrogen was monitored from its adsorption site. Finally, the lateral position of the dissociating hydrogen atom is defined by the variable λ_H, which is set equal to 1.0 if the hydrogen is at its adsorption site 2'. We set $\lambda_H = 0.0$ for the case where the hydrogen atom is placed at the free molecule's equilibrium in-plane distance Δy from the nitrogen atom along the y-direction. For each given combination of the parameters λ_N, z_N, and λ_H, the total energy was computed by relaxing the remaining degrees of freedom, including the z-coordinate of the dissociating hydrogen atom. For all other atoms in the surface region, including the two hydrogen atoms of the NH_2 group, no constraints were imposed on the relaxation.

The minimum energy path was determined by computing the total energy on a grid of the parameters λ_N, λ_H, and z_N. Figure 2 summarizes the result of these calculations. For distances $z_N \geq 0.8$Å, the hydrogen atom remained bonded to the molecule. The large energy difference between the two points at $z_N = 0.7$Å showed that the nitrogen atom reached its adsorption site simultaneously with the dissociation of the hydrogen atom, which started to approach its chemisorption site. Since a parameterized representation of the reaction pathway was used, not all degrees of freedom of the molecule were taken into account. In addition, dynamical effects were not included. Therefore, the energy barrier of 0.5 eV estimated from Fig. 2 was an upper bound for the dissociative adsorption of NH_2 and H on the vacancy $p(2\times2)$ reconstruction of the GaN($000\bar{1}$) surface.

References

1. V.M. Torres, M. Stevens, J.L. Edwards, D.J. Smith, R.B. Doak, and I.S.T. Tsong, Appl. Phys. Lett. **71**, 1365 (1997).
2 O.F. Sankey and D.J. Niklewski, Phys. Rev. B **40**, 3979 (1989).
3 A.A. Demkov, J. Ortega, O.F. Sankey, and M.P. Grumbach, Phys. Rev. B **52**, 1618 (1995).
4 J.E. Northrup, R. Di Felice, and J. Neugebauer, Phys. Rev. B **56**, R4325 (1997).
5 M.M. Sung, J. Ahn, V. Bykov, J.W. Rabalais, D.D. Koleske, and A.E. Wickenden, Phys. Rev. B **54**, 14652 (1996).
6 A.R. Smith, R.M. Feenstra, D.W. Greve, J. Neugebauer, and J.E. Northrup, Phys. Rev. Lett. **79**, 3934 (1997).
7 B. Daudin, J.L. Rouviere, and M. Arlery, Appl. Phys. Lett. **69**, 2480 (1996).
8 F.A. Ponce, D.P. Bour, W.T. Young, M. Saunders, and J.W. Steeds, Appl. Phys. Lett. **69**, 337 (1996).

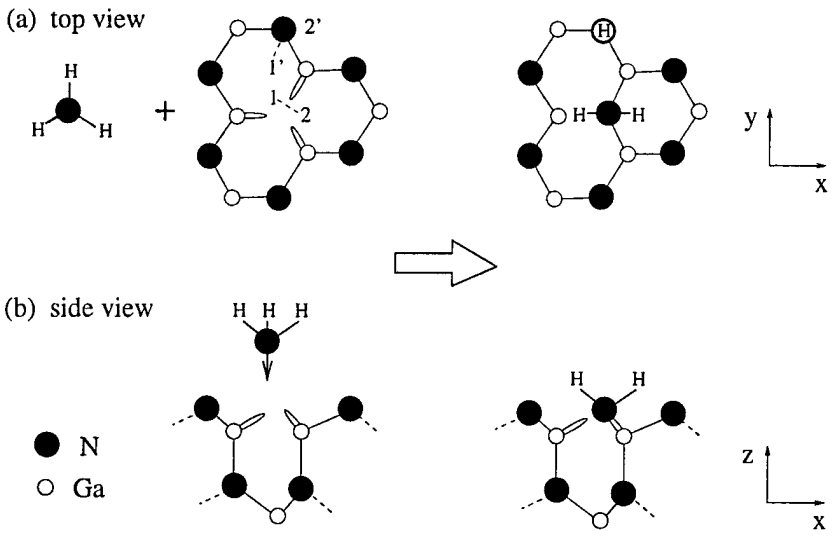

Figure 1: Schematic representation of a low energy-barrier pathway for the dissociative adsorption of ammonia at the $p(2\times2)$ vacancy structure of the GaN(000$\bar{1}$) surface. The molecule approaches the surface with its nitrogen atom above position 1 and with an orientation as illustrated in the top and side views. The molecule's hydrogen atom above position 1' is closest to a first-layer nitrogen atom. During the dissociation, the molecule's nitrogen atom moves closer to the surface and from position 1 to 2, while the separating hydrogen atom moves from position 1' to its bonding site 2' at the first-layer atom. The H atom chemisorbed on the surface atom is not pictured in the side view.

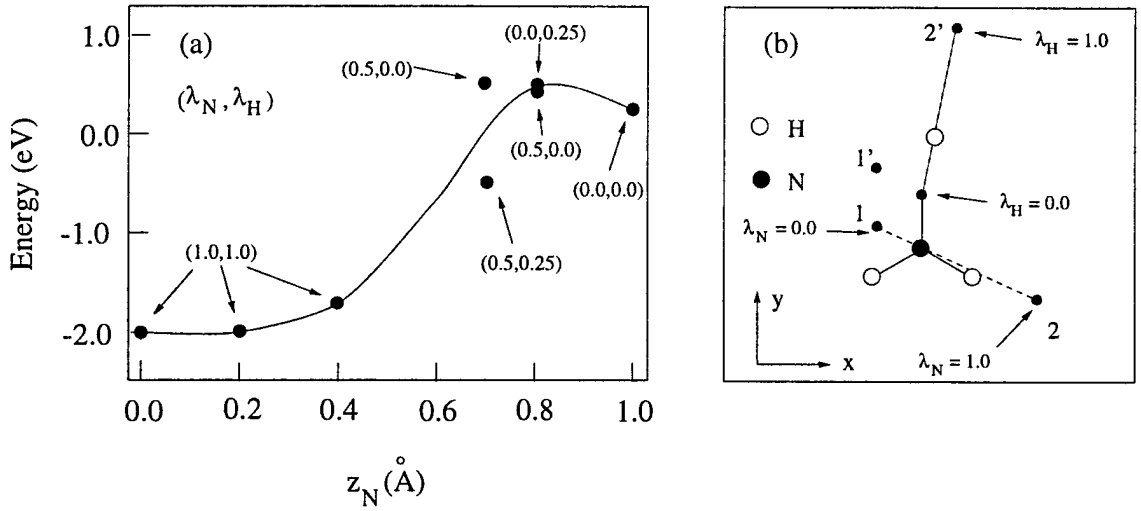

Figure 2: (a) Potential energy for ammonia approaching the nitrogen-vacancy structure of the GaN(000$\bar{1}$) surface along the minimum reaction energy path. The optimal parameters λ_N and λ_H for each value of z_N are given in parentheses. (b) Illustration of the parameters used to describe the dissociative chemisorption process. The labels 1,1',2, and 2' correspond to those of Fig. 1.

IV. Effects of Energy and Angle of Incidence on AlN and GaN Epitaxial Growth using Helium Supersonic Beams Seeded with NH_3

A. Introduction

The nitride family of AlN, GaN and InN thin films have shown to be strong candidates for electronic and optoelectronic applications. With direct band gaps of 6.2 eV, 3.4 eV and 1.9 eV for AlN, GaN and InN respectively, solid solutions based on these materials can provide band gap modifications suitable for applications ranging from the red to the deep UV region of the spectrum [1]. Due to the high bond strength between N and H in NH_3, the growth of III-V nitrides requires high substrate temperatures unless some other form of activation is present. Supersonic molecular beam epitaxy (SMBE) has been shown to enhance the surface decomposition of silane and methane [2,3] because of the possibility of tuning the kinetic energy of these species to deform and cleave the bonds upon impact with the substrate. In addition, the tuning of the energy spread is possible with SMBE. This is important in order to experimentally determine the chemisorption barriers for the systems being studied, as well as to provide species with high sticking coefficients at high enough intensities. Supersonic molecular beam epitaxy is, therefore, a useful technique for the low-temperature growth of single-crystalline GaN films at suitable growth rates using NH_3. A review of supersonic molecular beams can be found in Scoles [4].

Growth of stoichiometric, smooth epitaxial AlN and GaN films on 6H-SiC(0001) was accomplished using He supersonic beams seeded with NH_3. The dependence of the film properties on the kinetic energy and angle of incidence of the beam with respect to the surface normal of the substrate was studied. The growth of AlN films on SiC substrates as received and hydrogen-etched SiC substrates at 1600°C was also studied.

B. Experimental Procedure

The deposition chamber used for the current deposition experiments is the same deposition chamber used for previous MBE work at ASU [Sep. 97 Progress Report]. The samples were resistively heated by passing a current through them and the temperature was measured using a disappearing filament pyrometer. The temperatures of the Al and Ga evaporators were also measured with the pyrometer and set at 1110°C and 1010°C, respectively. In the present study, the substrates were on-axis 6H-SiC(0001) purchased from Cree research. The substrates were degreased by rinsing in methanol, acetone and isopropanol at 60°C for 5 min. The substrates were then sonicated in DI water for five min. followed by a dip in a 10% HF aqueous solution for 15 min. The samples were then loaded into the deposition chamber and the chamber was evacuated and baked such that a base pressure $< 8\times10^{-9}$ Torr was obtained. A liquid nitrogen trap was then filled to obtain a base pressure $< 7\times10^{-10}$ Torr. The evaporators were degassed

by gradually heating them to the operating temperatures while maintaining a pressure of $< 1\times10^{-8}$ Torr. The sample was then degassed by heating to ~ 500°C while the pressure in the chamber was maintained at $< 5\times10^{-9}$ Torr. The samples were then annealed at 900°C for 20 min. At this point, the isolation valve between the source chamber and the deposition chamber was opened such that the NH_3 seeded He beam impinged on the sample. The shutter on the Al evaporator was also opened and growth of AlN was performed for 60 min. After the deposition of AlN was completed, the sample temperature was set at 800°C and the Ga evaporator was opened. Deposition of GaN was carried out for 60 min. The films were characterized using Auger electron spectroscopy (AES), Rutherford back-scattering spectroscopy (RBS), scanning electron microscopy (SEM), electron channeling patterns (ECP) and atomic force microscopy (AFM).

C. Results

Although over thirty films have been grown over the last three months, not all the characterization results have been analyzed and understood. In general, the GaN layers exhibited ion channeling when analyzed by RBS indicative of their good crystallinity and epitaxy. The epitaxial nature of the films was further confirmed using ECPs. This is consistent with previous results [03/97 progress report]. An AES depth profile revealed a sharp, clean interface between the AlN film and the SiC substrate. SEM analysis revealed that the films were smooth and continuous. Preliminary AFM results revealed an RMS roughness of ~ 10 nm over an area of 10 μm × 10 μm for the GaN layers.

Also examined was the effect of kinetic energy on the growth kinetics of GaN layers. Figure 1 shows a plot of the film thickness as a function of kinetic energy perpendicular to the surface. For the lowest energy used, 0.031 eV, the film thickness was comparable to that of the films grown with energies greater than 0.33 eV. The growth rate showed a decrease as the energy increases from 0.031 eV to 0.061 eV. Increasing the kinetic energy from 0.061 eV to 0.33 eV showed a sharp increase in growth rate. For kinetic energies greater than 0.33 eV, the growth rate seemed to be constant. Johnston *et al.*[5] observed that for low energy supersonic beams the growth rate decreased with increasing kinetic energy. Previous work [December, 1996 progress report] showed a sharp increase in growth rate when increasing the kinetic energy from 0.22 to 0.40 eV. The general form of the curve shown in Fig. 1 was also exhibited in sticking probability measurements for Cl_2 on Si(100)-(2×1) surfaces [6]. The fact that considerable growth rates were obtained at low kinetic energies suggests the existence of a physisorption well where low energy ammonia molecules can be accommodated. The decrease in film thickness as the kinetic energy increased from 0.031 to 0.061 eV, was due to increased desorption from the physisorption well. As the energy increases from 0.061 to 0.33 eV, the molecules became energetic enough to overcome the chemisorption barrier and the growth rate

increased. Once the kinetic energy was comparable to the chemisorption barrier, the growth rate became independent of kinetic energy. Following this interpretation for the data in Fig. 1, it was proposed that the barrier height for dissociative chemisorption must be approximately 0.3±0.1 eV. It is important to note that this was the first time that such barrier was measured experimentally. Chiang *et al.* [7] found that NH_3 dissociatively chemisorbs on polycrystalline clean or H-terminated GaN. Shekhar and Jensen [8] found that the decomposition of NH_3 on single crystal GaN surfaces led to the formation of surface NH_2 and H. Fritsch *et al.* [9] calculated the barrier of 0.50 eV for NH_3 dissociative chemisorption on GaN using molecular dynamics simulations. Results from this laboratory are in agreement with the existence of a dissociative chemisorption path as well as the magnitude of its barrier height.

Even though the data obtained during the past three months has not been fully analyzed, RBS channeling results showed that AlN films grown on hydrogen-etched SiC substrates were superior to those grown on "as received" substrates.

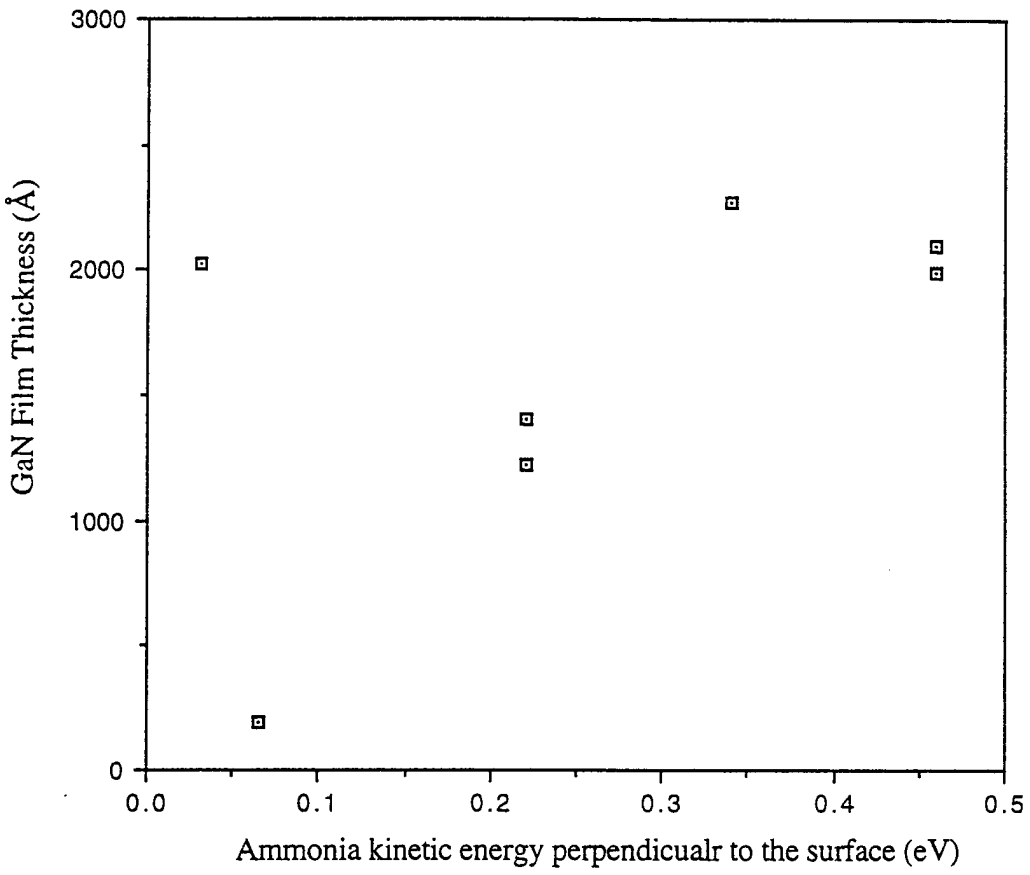

Figure 1. Film thickness as a function of ammonia kinetic energy for normal incidence beams.

D. Conclusions

The growth rate dependence of epitaxial GaN films on NH_3 kinetic energy was studied. Ammonia physisorbed on the surface at low kinetic energies (i.e.. 0.031-0.061 eV) and started to dissociatively chemisorb with increasing kinetic energy. For kinetic energies greater than 0.33 eV, the growth rate remained constant, which suggested that the barrier for dissociative chemisorption was overcome. From these observations, it has been proposed that the barrier height is approximately 0.3±0.1 eV.

Preliminary results suggested that AlN films grown on hydrogen-etched SiC substrates were superior to those grown on as-received SiC substrates.

E. Future Work

In the next three months, work will continue on analyzing the films grown over the past three months. Some of the work with varying angle of incidence appeared to show that for a beam oriented 30° away from the surface normal, the growth rate decreased for increasing total kinetic energy in the range of 0.22 to 0.46 eV. Continued work along these lines will be performed to understand the conditions present during depositions in the LEEM using the supersonic beam. Growth of GaN on the AlN layers on the hydrogen-etched substrates will be continued.

F. References

1. S. Strite and H. Morkoc, J. Vac. Sci. Technol. **B10**, 1237 (1992)
2. M.E. Jones, L.Q. Xia, N. Maity, J.R. Engstrom, Chem. Phys. Lett. **229**, 401 (1994)
3. S.T. Ceyer, J.D. Beckerle, M.B. Lee, S.L. Tang, Q.Y. Yang, M.A. Hines, J. Vac. Sci. Technol. A **5**, 501, (1987)
4. D.R. Miller, *Atomic and Molecular Beam Methods*, Ch. 2, Ed. G. Scoles, Oxford University Press (1988)
5. A.M. Johnston, D.E. Crawford, R. Held, A.M. Dabiran and P.I. Cohen, SEE I & II workshops, sponsored by the Office of Naval Research (1995, 1996)
6. D. J. D. Sullivan, H.C. Flaum and A.C. Kummel, J. Phys. Chem. **97**, 12051 (1993)
7. C.-M. Chiang, S.M. Gates, A. Bensaoula, J.A. Schultz, Chem. Phys. Lett. **246**, 275 (1995)
8. R. Shekhar and K.F. Jensen, Surf. Sci. **381**, L581 (1997)
9. J. Fritsch, O.F. Sankey, K.E. Schmidt and J.B. Page, submitted for publication to Phys. Rev. B.

V. Homoepitaxial Growth of GaN Films Using an NH_3-seeded Supersonic Beam

A. Introduction

Gallium nitride is a wide band gap semiconductor (Eg=3.4 eV) with many potential optoelectronics and high-temperature, high-frequency, microelectronics applications. Gallium nitride forms a continuous range of solid solutions with AlN (6.28 eV) and InN (1.95 eV), permitting the fabrication, via band gap engineering, of laser diodes with tunable emission frequencies from covering the visible and UV regions. State-of-the-art GaN films ($\leq 10^8$ defects per cm^2) have been used to fabricate blue light emitting diodes (LEDs) and laser diodes.

Heteroepitaxial growth of high-quality monocrystalline GaN films has been problematic due to the lack of a suitable lattice-matched substrate and the thermodynamic instability of GaN under high-temperature growth conditions. Sapphire, the most common substrate, exhibits a 14% lattice mismatch at the GaN(0001)/sapphire(0001) interface; moreover, the thermal expansion coefficient of sapphire is 25% greater than that of GaN. Only by employing a low-temperature AlN or GaN buffer layer can one obtain monocrystalline GaN films on sapphire with defect densities in the 10^8–10^9 cm^{-2} range.

Substrate temperatures in excess of 1000°C are employed for growth of monocrystalline GaN films by halide or metal-organic CVD (MOCVD) using NH_3. In MOCVD, substrate thermal energy is used to overcome activation barriers for precursor decomposition and adatom surface migration (lateral diffusion); however, GaN decomposition above 620°C *in vacuo* necessitates the use of large V/III flux ratios [1]. Plasma-assisted processes have been utilized to lower the GaN growth temperature to approximately 700°C, but ion-induced damage and oxygen contamination are often observed.

The use of energetic neutral beams of precursor molecules is an alternative approach to the epitaxial growth of GaN films at lower substrate temperatures. In selected energy epitaxy (SEE), heavy reactant molecules are seeded in a supersonic expansion of light molecules and thereby accelerated to hyperthermal energies. The precursor molecules attain kinetic energies on the order of 1-2 eV which can provide the necessary energy for activated surface processes, such as dissociative chemisorption and adatom migration. Hence, in prospect, monocrystalline GaN films may be grown at lower substrate temperatures by SEE than by conventional MOCVD [2]. Moreover, energetic neutral beams with narrow energy distributions are ideal tools for fundamental studies of wide band gap semiconductor growth using *in situ* low-energy electron microscopy (LEEM) and other techniques.

To demonstrate the potential advantages of SEE, homoepitaxial growth of GaN was investigated obviating the substrate lattice-mismatch issue and allowing the effects of precursor kinetic energy and film morphology to be studied in isolation. In this work, the effects of

substrate temperature, Ga flux, NH_3 flux, and NH_3 kinetic energy on GaN growth kinetics and surface morphology were investigated using a seeded supersonic NH_3 beam and Ga effusion cell. In addition, secondary ion mass spectroscopy (SIMS) analysis was performed on selected films to determine the concentrations of C, O, and Si impurities.

B. Experimental Procedure

SEED/XPS Deposition System. The SEED/XPS multi-chamber system described in previous reports (June 1996, Dec. 1996) was used for homoepitaxial growth of GaN. The orifice used in the NH_3 nozzle was 150 mm. A conical skimmer used for extracting the NH_3 beam from the supersonic free jet had an opening of 1 mm in diameter, a base of 20 mm in diameter, an included angle of 25° at the opening and of 70° at the base, and a height of 17 mm. The collimation aperture of 5×5 mm^2 was located downstream between the 2nd differential pumping stage and the growth chamber. The molecular beam was directed to the substrate with an incident angle of 6° with respect to the surface normal. The deposition area on the vertical substrate was 15×15 mm^2.

Substrate Preparation/Cleaning. The substrates were 2-μm thick GaN films grown by MOVPE on on-axis 6H-SiC employing a 0.1-μm thick AlN buffer layer. The substrates were provided by M. Bremser and O. Nam of the Davis group and used as received. Ag paste was used to provide good thermal contact between the Mo sample holder and the GaN/AlN/6H-SiC substrate; two Mo pins were used to hold the substrate in place. The Mo holder was placed on a hot plate to dry the Ag paste for 5 min at 80°C. Subsequently, it was introduced via the load-lock chamber and transferred *in vacuo* into the growth chamber. The sample was heated slowly to 400°C under an NH_3 flux for outgassing. Prior to the growth, the GaN substrate was cleaned *in situ* by NH_3 beam exposure at 730°C for 30 min, unless otherwise noted. After *in situ* cleaning the substrate temperature was lowered to 200°C under an NH_3 flux. The GaN substrate was examined by RHEED before and after *in situ* cleaning to ensure that the surface was clean prior to growth.

Homoepitaxial Growth Using Supersonic NH_3 Beam and Ga Effusion Cell. A hot-lip Ga Knudsen cell (K-cell) described in a previous report (June 1997) was used for the homoepitaxial growth of GaN. Films were grown using the Ga cell and a NH_3-seeded supersonic molecular beam. Growth was initiated by opening the K-cell shutter after both the Ga crucible and the substrate were at the desired temperatures. Growth runs lasted for two hours, unless otherwise noted. Many of the growth experiments were with the NH_3 nozzle heated to 200°C and the stagnation pressure in the 745-755 Torr range, employed a NH_3 flow rate of 60 sccm and a He flow rate of 200 sccm. Changes in the NH_3 kinetic energy were made by changing the nozzle temperature, 25°C-600°C, or the NH_3 flux, 30 or 60 sccm. Gallium nitride growth experiments were done in the substrate temperature range of 730–770°C. The

Ga K-cell temperatures ranged from 950°C to 1050°C. Growth rates were determined by profilometer measurement of the step height of the film created by the pins holding the substrate, and it was referenced to the cross sectional SEM images.

XPS Analysis. The UHV surface analysis chamber was equipped with a PHI 3057 XPS system comprising a 10-360 spherical capacitor analyzer (SCA), Omni Focus III fixed-aperture lens, 16-element multichannel detector, and 257 DR11 PC interface card. A PHI 1248 dual-anode (Al/Mg) X-ray source was used. The sample was mounted on a tilt stage which was attached to a precision *xyz*-rotary manipulator (Thermionics). The analysis chamber was pumped by a Perkin-Elmer TNBX ion pump/TSP combination and had a base pressure of 8×10^{-11} Torr. After growth, samples were transferred to the XPS chamber through vacuum transfer lines. XPS spectra were taken with both Mg and Al anodes to isolate N(1s), O(1s), C(1s) and Ga($2p_{3/2}$) photoelectron peaks from other interfering signals.

RHEED. In situ reflection high-energy electron diffraction (RHEED) measurements were made using a Fisons LEG 110 15-kV electron gun and 100-mm Al-coated phosphor screen. RHEED patterns of the GaN substrate before and after the *in situ* cleaning, and after GaN growth were taken at 15kV.

SEM. Scanning electron microscope images of GaN films were obtained using a JEOL 6400FE SEM with a 5-kV cold field emission electron gun. Both surface and cross sectional images were taken.

AFM. The AFM images were obtained using a Digital Instruments Dimension 300 Scanning Probe Microscope with a Nanoscope IIIa Controller. A silicon tip with a nominal tip radius of curvature of 5-10 nm was used.

SIMS. SIMS depth profiles were measured using a Cameca IMS-6f with a mass resolution of 25000M/ΔM. A Cs^+ primary ion beam was used.

C. Results and Discussion

Homoepitaxial Growth Using Supersonic NH_3 Beam and Ga K-cell. Growth runs were conducted at substrate temperatures of 730°C and 770°C with Ga K-cell temperatures of 900°C to 1050°C. The growth conditions, growth rates, and AFM-determined RMS surface roughness values of the films are summarized in Table I.

The average NH_3 kinetic energy $\langle E_K \rangle$ was estimated from the mixture composition and nozzle temperature (T_0) assuming perfect gas behavior, zero velocity slip between the heavy and light species and an infinite terminal Mach number [3]. The terminal kinetic energy of species *i* in a mixed gas expansion of average molecular weight, W_{ave}, is given by:

$$\langle E_i \rangle = \frac{W_i}{W_{ave}} \frac{\gamma R T_0}{(\gamma - 1)}$$

where γ, R and W_i are the molar heat capacity ratio C_p/C_v, the gas constant, and the molecular weight of species *i*, respectively. The kinetic energy of the seeded NH_3 is seen to increase with T_0 and increasing dilution of the NH_3 in the lighter bath gas, He.

The GaN homoepitaxial growth rate at substrate temperatures of 730°C and 770°C is shown in Fig. 1 as a function of incident Ga flux. The growth rate is expressed as a net Ga incorporation flux. The incident Ga flux was estimated using the Knudsen cell temperature and growth chamber geometry, assuming a ideal effusive source [4].

$$J(\varphi) = 1.1\times10^{22}\left[\left(AP/d^2\right)(MT)^{-1/2}\right]\cos\varphi \text{ molecules cm}^{-2}\text{s}^{-1}$$

Where A, P, d and φ are K-cell orifice area, equilibrium vapor pressure in the cell at temperature T, distance from the source and substrate and angle between cell axis and the normal to the substrate surface, respectively. A linear relationship was observed for incident Ga fluxes $\leq 1.2\times10^{15}$ $cm^{-2}s^{-1}$, indicative of Ga-limited growth. Moreover, the GaN growth rate was nearly independent of substrate temperature under these conditions. From the slope of the relationship in Fig. 1, a Ga incorporation efficiency of 20-25% was estimated.

The dependence of the GaN growth rate on NH_3 beam conditions (flux and kinetic energy) is illustrated in Fig 2. The films were grown using a substrate temperature of 730°C and an incident Ga flux of 4.5×10^{14} $cm^{-2}s^{-1}$ (Ga K-cell 950°C). The effect of reducing the

Table I. Homoepitaxial Film Growth Conditions, Growth Rate and RMS Roughness

Film	Growth Temp (°C)	Ga K-cell Temp (°C)	NH_3 Flowrate (sccm)	Nozzle Temp (°C)	Growth Rate (nm/h)	RMS (nm)
82597	730	900	60	200	57	NA
121697	730	950	60	25	104	14
100897	730	950	60	200	98	19
101197	730	950	30	200	94	14
101397	730	950	60	600	105	24
101497	730	950	30	600	109	32
101797	730	970	60	200	136	NA
102497	730	1000	60	200	233	NA
121597	770	970	60	200	165	32
101097	770	1000	60	200	240	NA
102597	770	1050	60	200	426	31
103097	770	1050	30	200	427	28
103197	770	1050	30	600	428	32

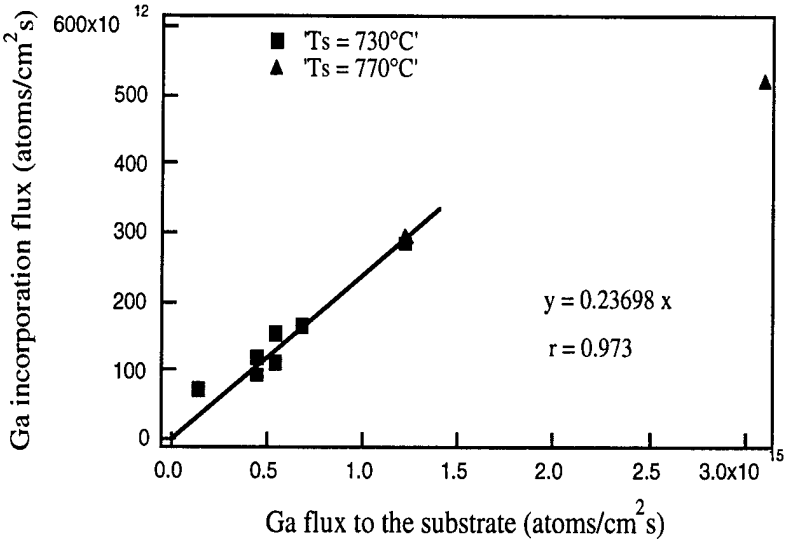

Figure 1. Relationship between incident Ga flux and GaN growth rate. NH_3 beam conditions: 23% NH_3 in He with a nozzle temperature of 200°C.

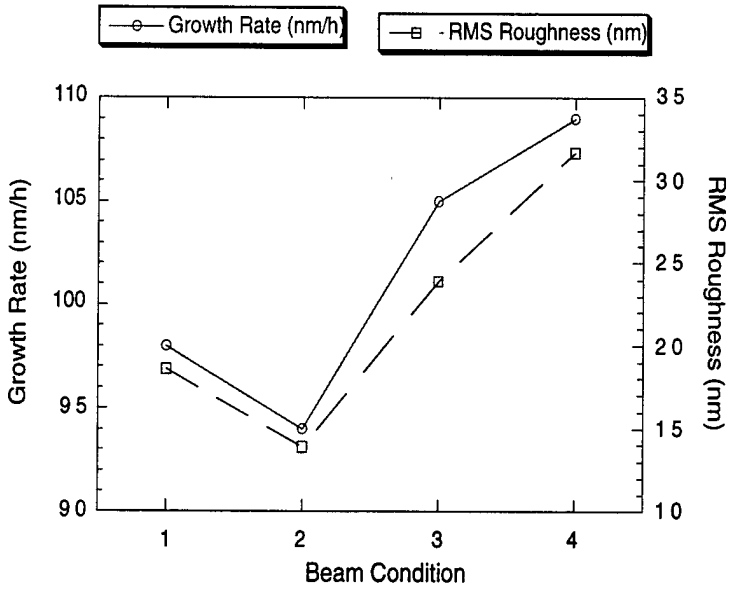

Figure 2. Dependence of GaN growth rate and film morphology on NH_3 beam conditions. Growth conditions: 730°C substrate temperature, 4.5×10^{14} $cm^{-2}s^{-1}$ incident Ga flux.

NH_3 kinetic energy by approximately 30% is to lower the GaN growth rate by less than 5%. Increasing the NH_3 kinetic energy by a factor of 1.8 at low NH_3 flux results in an increase in growth rate of 16%. In contrast, increasing the NH_3 kinetic energy by a factor of 1.8 at high NH_3 flux results in an increase in growth rate of 7%. The data are consistent with enhancement of NH_3 reactivity with increasing kinetic energy in the 0.25 to 0.61 eV range.

Atomic force microscopy (AFM) scans of films grown at 730°C using NH_3 beams with properties corresponding to Conditions 2 and 4 in Table II are shown in Figs. 3 and 4.

Table II. Properties of NH_3-Seeded Supersonic Molecular Beams

Condition	1	2	3	4
% NH_3	23	10	23	10
Nozzle Temp (°C)	200	200	600	600
$\langle E_K \rangle$ (eV)	0.25	0.33	0.46	0.61

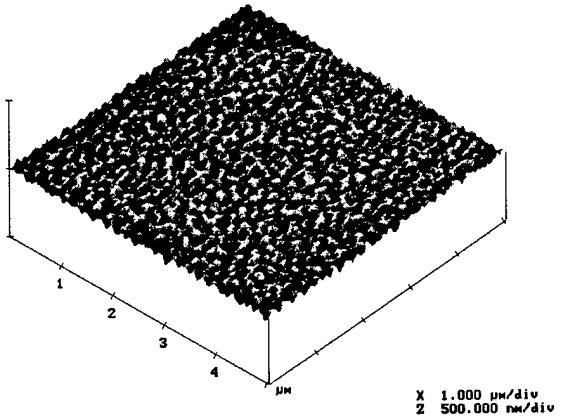

Figure 3. AFM picture of Condition 2 film in Table I.

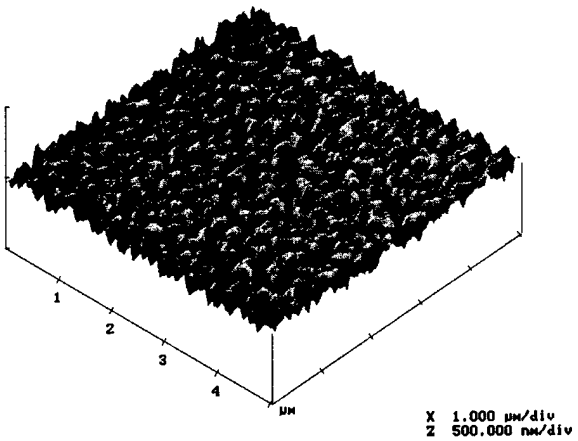

Figure 4. AFM picture of Condition 4 film in Table I.

Rough surface morphologies are observed; however, the film grown using the low kinetic energy NH_3 beam (Fig. 3) is markedly smoother than the one grown using a high kinetic energy beam (Fig. 4). The RMS roughness values are observed to correlate well with the trends in GaN growth rate as seen in Fig. 2. From these results, we infer that the increased surface roughness observed at higher NH_3 kinetic energies is related to the increase in NH_3 reactivity. Smoother films are obtained by using a lower NH_3 flux and/or NH_3 kinetic energy, thereby increasing the Ga species surface diffusion length.

In contrast, films grown at 770°C (1050°C K-cell temperature) under different NH_3 flux and/or NH_3 kinetic energy conditions (Table I) had equivalent growth rates and similar RMS roughness values. The growth rates are >0.4 μm/h, and the films exhibit a rough "peak-and-valley" surface morphology, as illustrated by the AFM image in Fig. 5. The higher substrate temperature and Ga flux appear to negate the effects of NH_3 kinetic energy on growth rate and film morphology.

SIMS Analysis. On-line XPS of the GaN films shows surface contamination of 5-16 atomic % carbon and 3-11 atomic% oxygen, as detailed in previous reports (September 1997). The impurity concentrations in the substrate and the homoepitaxial GaN film were examined by SIMS analysis. Substrate carbon, oxygen and silicon concentrations are $2\text{-}3\times10^{15}$, 1×10^{16} and 1×10^{18} atoms/cm^3, respectively. Carbon and oxygen concentrations of 7×10^{17} atoms/cm^3 are observed in a homoepitaxial GaN film grown at 770°C using a 1050°C Ga K-cell temperature. Thus, the carbon and oxygen concentrations in the film are 4000 times less than observed at the surface. This indicates that surface contamination results not from the growth process but from contamination acquired during cool-down after growth or transfer to the XPS chamber.

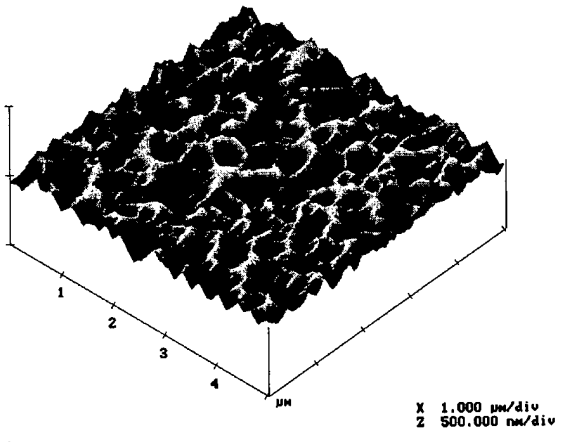

Figure 5. AFM image of GaN film grown at 770°C and 1050°C Ga K-cell temperature using 0.25 eV-NH_3 beam (Condition 1).

The SIMS results show that there was a problem with Si contamination during growth. Depth profiles showed that the atomic concentration of Si in the film is 6×10^{19} atoms/cm^3, which was large enough to affect GaN film morphology. The most probable source of Si contamination was from the diffusion pump oil in the SEE source chamber, which may diffuse into the growth chamber via the TEG beam aperture, since the TEG nozzle was not used during GaN deposition with the K-cell. Future growth runs will be performed using a 200 sccm He flow through the TEG nozzle. The diffusion pump oil (DC 704) will also be replaced with a lower vapor pressure oil (DC 705). SIMS analysis of the resultant films will be done to determine if the Si contamination problem has been eliminated.

E. Future Plans

The sources of carbon, oxygen, and silicon impurites in the GaN films will be identified and eliminated. Films will be grown using a He flow through the TEG nozzle, and SIMS analysis will be done to determine if the Si contamination source is the diffusion pump oil.

A detailed investigation of GaN homoepitaxial growth using dual NH_3 and TEG supersonic beams will be done to elucidate the relationships between film quality and precursor kinetic energies tuned by seeded supersonic beams.

Time-of-flight (TOF) velocity measurements will be made in order to establish velocity and kinetic energy distributions of the seeded supersonic molecular beams.

A radio-frequency discharge nozzle/nitrogen atom source [5,6] will be constructed and installed in the system. This source will produce a supersonic beam of atomic nitrogen and will be used in conjunction with the TEG supersonic source and the Ga K-cell for GaN growth.

Real-time RHEED intensity measurements will be used to investigate the growth mode of GaN epilayers using a CCD camera-based data acquisition system.

A major upgrade of the SEE vacuum system will be completed in the Spring of 1998.

F. References

1. S. Nakamura, Japan. J. Appl. Phys. **30**, L1705 (1991).
2. M. R. Lorenz and B. B. Binkowski, J. Electrochem Soc. **109**, 24 (1962).
3. D. R. Miller in *Atomic and Molecular Beam Methods*, Ch. 16, Ed. G. Scoles, Oxford University Press (1998).
4. K. Ploog in *Atomic and Molecular Beam Methods,* Ch. 16, Ed. G. Scoles, Oxford University Press (1998).
5. C. B. Mullins, Appl. Phys. Lett. **68**, 3314 (1996).
6. J. E. Pollard, Rev. Sci. Instrum. **63**, 1771 (1992).

VI. Distribution List

Dr. Colin Wood Office of Naval Research Electronics Division, Code: 312 Ballston Tower One 800 N. Quincy Street Arlington, VA 22217-5660	3
Administrative Contracting Officer Office of Naval Research Regional Office Atlanta 100 Alabama Street, Suite 4R15 Atlanta, GA 30303	1
Director, Naval Research Laboratory ATTN: Code 2627 Washington, DC 20375	1
Defense Technical Information Center 8725 John J. Kingman Road, Suite 0944 Ft. Belvoir, VA 22060-6218	2